Realistic Assessment of Spectrum Sensing for TV White Space Scenarios in Brazil: Insights for System Optimization

André A. Anjos, Dayane C. J. Martins, Rausley A. A. de Souza

***Abstract*— The need for ever-higher transmission bands in the most advanced telecommunications systems is primarily brought on by the growing traffic demand from new services and applications aimed at their consumers. These new systems are currently having trouble accessing the necessary bands because of a situation of spectral scarcity. However, the electromagnetic spectrum's physical constraints are only one cause of this scarcity; another is the spectrum's underutilization. Cognitive radios, which have spectral sensing capabilities, appear to be a solution to this underutilization issue. This paper assumes scenarios of transmission opportunities inside the TV White Space spectrum in Brazil to simulate and assess spectral sensing based on the energy detection technique. The implemented simulation considers the licensed users' use of an OFDM-like transmission signal in this frequency band, which has clearly defined and standardized features. Through the investigation of detection and false alarm probability, the study evaluates how effectively the spectrum sensing system performs in various circumstances.**

***Keywords*— TV White Spaces, Spectrum Sensing, Energy Detection, ISDB-T$_B$.**

I. Introduction

Nowadays, the desire for connectivity and high data rates has fueled the creation of ever-more-advanced telecommunications infrastructure [1]. However, the development and deployment of these new systems have encountered a major problem, which is the shortage of electromagnetic spectrum [2]. Analyses by different authors around the world have shown that the current spectrum scarcity scenario arises not only from a physical limitation of the electromagnetic spectrum but also from its underutilization [3], largely due to the current fixed spectrum allocation policy, which becomes more evident in the VHF (Very High Frequency) and UHF (Ultra High Frequency) bands, which are intended for TV channel allocation.

André A. dos Anjos, Universidade Federal de Uberlândia (UFU), Patos de Minas, e-mail: andre.anjos@ufu.br; Dayane. C. J. Martins, Universidade Federal de Uberlândia (UFU), Patos de Minas, e-mail: dayane.martins@ufu.br; Rausley A. A. de Souza, Instituto Nacional de Telecomunicações (INATEL), Santa Rita do Sapucaí, e-mail: rausley@inatel.br. This work was partially supported by CNPq (Grant References 311470/2021-1 and 403827/2021-3), by São Paulo Research Foundation (FAPESP) (Grant No. 2021/06946-0), and by RNP, with resources from MCTIC, Grant No. 01245.020548/2021-07, under the Brazil 6G project of the Radiocommunication Reference Center (Centro de Referência em Radiocomunicações - CRR) of the National Institute of Telecommunications (Instituto Nacional de Telecomunicações - Inatel), Brazil, and by Huawei, under the project Advanced Academic Education in Telecommunications Networks and Systems, contract No PPA6001BRA23032110257684.

The unused spaces of the TV spectrum have become known worldwide as TV White Spaces (TVWS) and are emerging, along with a new policy of dynamic spectrum allocation called Dynamic Spectrum Access (DSA), as a solution to overcome this "scarcity" problem, making its use more efficient. Recently, the board of directors of the National Telecommunications Agency (ANATEL) in Brazil approved a proposal to regulate the dynamic use of idle TVWS spectrum by secondary users [4]. The approved resolution proposal assigns and designates VHF and UHF bands for this type of application, initially considering the 54-72 MHz, 174-216 MHz, 470-608 MHz, and 614-698 MHz bands. The regulation on usage conditions is still under development, and the expectation is that it will provide for the use of idle TV bands for mobile cellular and broadband services. Regional providers have already expressed interest in using TVWS in a secondary capacity using LTE and 5G, although they acknowledge that there is still no scale of appropriate equipment for opportunistic use of idle spectrum.

In this context, it is necessary to study and develop increasingly intelligent radios equipped with new technologies that can efficiently utilize this available resource. These intelligent radios are called cognitive radios (CRs), which are telecommunications devices capable of making dynamic decisions based on information collected in the environment in which they are located [5]. The main functionality of a CR that promises to solve the problem of electromagnetic spectrum scarcity is spectral sensing which is the focus of this work.

Several studies in the field of spectral sensing address different scenarios and use different implementation techniques. For example, the authors in [6] present research containing an overview of cognitive radio architectures and spectral sensing techniques such as matched filtering, energy detection, and cyclostationary detection. The authors in [7] present work on spectral sensing with multiple antennas using likelihood ratio detection and power spectral density division cancellation. The authors of [8] present research on spectrum detection based on a composite neural network, aiming to improve the intelligence level of CR and thus upgrade the performance of sensing techniques. However, despite the various scientific works, there is a lack of studies that address more realistic simulations of spectral sensing techniques. Thus, the main objective of this article is to provide a deeper understanding of spectral sensing in a TVWS scenario in Brazil, with a simulated implementation that closely resembles a practical situation. The simulation and the study addressed in this work stand out for the following contributions: (i) the considered

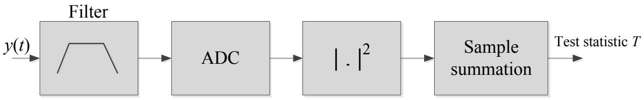

Fig. 1. Block diagram of the energy detection technique.

primary user signal (PU) is compliant with the Brazilian Digital TV standard; (ii) the sampling frequency used in the simulations was carefully selected for sensing a 6 MHz TV channel; (iii) a pessimistic sensing scenario is also considered, in which the CR is in a non-line-of-sight (NLOS) scenario; (iv) conclusions are drawn regarding the influence of system parameters on sensing. The simulation will serve as a basis for future hardware implementation of spectral sensing in TVWS.

II. Spectrum Sensing in Cognitive Radios

A. Mathematical Modeling of a Spectral Sensing System

The model consists of two hypotheses that will be used for decision-making, namely H_0 and H_1. The H_0 hypothesis considers the absence of a primary signal in the sensed band, while the H_1 hypothesis refers to the presence of a PU signal in that same band. The two hypotheses can be mathematically described as

$$y(t) = \begin{cases} n(t), & \text{if } H_0 \\ h(t)x(t) + n(t), & \text{if } H_1 \end{cases} \tag{1}$$

where $y(t)$ is the signal captured and analyzed by the CR, $n(t)$ corresponds to the thermal noise in the receiver, $h(t)$ represents the gain or attenuation caused by the communication channel, and $x(t)$ is the PU transmitted signal. To perform the decision-making process regarding spectral occupancy, it is necessary to define a decision variable, T, generated by processing $y(t)$, which will depend on the sensing technique used, and also a decision threshold, λ. Thus, if $T > \lambda$, it is decided that the spectrum is occupied, otherwise, it is considered free.

B. Energy Detection Technique

There are several spectral sensing techniques available, among which cycle-stationary detection [9], matched-filter detection [10], and eigenvalue-based detection [11] can be cited. However, energy detection is currently the most widely used technique [12], [13], owing to its low implementation complexity. It is considered an optimal technique when no prior knowledge of the transmission signal is available, and the noise is not a source of uncertainty. In this technique, the detection of the presence or absence of the signal is based on monitoring the energy measured in the channel, compared to a decision threshold. Despite being a well-established sensing technique, nowadays it still attracts considerable attention from researchers worldwide [14], [15]. Fig. 1 depicts the block diagram for the implementation of the energy detection technique in the time domain. Following the block diagram shown in Fig. 1, a bandpass filter centered at the frequency of the channel of interest is first used. Subsequently, the filtered signal is down-converted to the baseband and then digitized by an analog-to-digital converter (ADC), generating samples that are squared. The decision statistic, T, is then calculated according to

$$T = \sum_{i=1}^{n} |y(i)|^2 , \tag{2}$$

where n is the total number of collected samples and $y(i)$ represents the i-th digitized sample collected by the CR. After the calculation of T, its value is compared with λ for decision-making about which of the two hypotheses, H_0 or H_1, will be considered. In the presence or absence of the primary signal, the decision variable has a chi-square distribution with n degrees of freedom [16]. Considering a sufficiently large number of samples, n, and using the central limit theorem, this variable can be approximated to a Gaussian random variable, $T = \mathcal{N}(n\sigma_\mathrm{w}^2, n\sigma_\mathrm{w}^4)$ under hypothesis H_0 and $T = \mathcal{N}(n(\sigma_\mathrm{s}^2 + \sigma_\mathrm{w}^2), n(\sigma_\mathrm{s}^2 + \sigma_\mathrm{w}^2)^2)$ under hypothesis H_1, and thus, the probabilities of false alarm and detection can be numerically resolved, given respectively by

$$P_\mathrm{fa} = Q\left(\frac{\lambda - n\sigma_\mathrm{w}^2}{\sqrt{n\sigma_\mathrm{w}^4}}\right), \tag{3}$$

$$P_\mathrm{d} = Q\left(\frac{\lambda - n(\sigma_\mathrm{s}^2 + \sigma_\mathrm{w}^2)}{\sqrt{n(\sigma_\mathrm{s}^2 + \sigma_\mathrm{w}^2)^2}}\right), \tag{4}$$

where σ_w^2 and σ_s^2 are the noise and PU signal variances, respectively; $Q(\cdot)$ is the Q-function, commonly used for solving problems involving numerical integration of area in Gaussian distributions. To define the threshold to be used, a constant false alarm rate value is used, which can be calculated by isolating λ in equation (3), and then

$$\lambda = \sigma_\mathrm{w}^2(Q^{-1}(P_\mathrm{fa})\sqrt{n} + n). \tag{5}$$

C. Primary User Signal in TV White Spaces in Brazil

The primary user signal considered in the spectral sensing simulations evaluated in this work is a transmission signal of OFDM (Orthogonal Frequency Division Multiplexing) type, fully compliant with the transmission signal of the Brazilian digital TV standard, the ISDB-$\mathrm{T_B}$ (Integrated Services Digital Broadcasting - Terrestrial Brazilian Version), whose characteristics are detailed in the ABNT 15601 [17] standard and can be mathematically described by

$$s(t) = \sum_{s=0}^{\infty}\sum_{k=0}^{K-1} c_{s,k}\psi(s,k,t) \tag{6}$$

$$\psi(s,k,t) = \begin{cases} e^{j2\pi\frac{k-K_\mathrm{c}}{T_\mathrm{u}}(t-T_\mathrm{g}-sT_s)} & sT_s \le t < (s+1)T_s \\ 0 & t < sT_s, t \ge (s+1)T_s \end{cases} \tag{7}$$

in which k is the index of the carrier, which is successive for the entire band, with the number 0 assigned to carrier 0 of segment 11; s is the symbol number; K represents the total carriers of the mode; T_s is the duration time of the OFDM symbol; T_g is the duration time of the guard interval; T_u is the duration time of the useful part of the symbol; f_c is the center frequency of the PU signal; K_c is the carrier number

TABLE I
OFDM ISDB-T$_B$ SYSTEM TRANSMISSION PARAMETERS.

Parameter	Value
Total number of carriers	8192 (Mode 3)
Number of active carriers	5617
Guard nterval	$1/32$
Number of segments Layer A	13
Data carriers modulation Layer A	64-QAM
Number of segments Layer A	13
Encoding rate of layer A	$7/8$
Pilot carriers and TMCC modulation	BPSK/DBPSK
OFDM symbol duration	1.26 ms
Subcarrier spacing	0.992 kHz
Pilot spacing	11.9 kHz
IFFT clock	$512/63$ MHz
BW	5.572 MHz

corresponding to the center frequency of the signal, and $c_{s,k}$ is the corresponding complex serial symbol to the OFDM symbol with index s and carrier index k.

With the theoretical knowledge of the ISDB-T$_B$ transmission signal, it will be possible to simulate the PU signal in compliance with the one that will be found in a real environment of spectral sensing in TVWS bands in Brazil.

III. Developments of Simulations

A. Generation of Primary User Signal in TVWS in Brazil

Before starting the development of spectral sensing simulations with a focus on TVWS usage, an OFDM signal in compliance with the characteristics of a typical ISDB-T$_B$ transmission signal was implemented in MATLAB. Table I presents the parameters used in this implementation of the OFDM signal, which will be incorporated into the spectral sensing simulations.

In the considered mode, we generate an OFDM signal by creating a vector consisting of 5617 complex random symbols that are structured in an OFDM frame. This frame structure includes data symbols (64-QAM), pilot symbols (BPSK), and TMCC symbols (DBPSK) in predetermined positions as per the ISDB-T$_B$ standard, which will later modulate each active carrier of the system. The transmission constellation of the active carrier symbols in the system is depicted in Fig. 2, where Q and I represent the imaginary and real parts of each symbol, respectively. Next, the symbol vector in the frame structure is parallelized for orthogonal frequency division multiplexing using the IFFT (Inverse Fast Fourier Transform) mathematical operation, generating a complex signal in the time domain with 8192 samples (mode 3) at the IFFT frequency, representing the useful OFDM symbol. A guard interval of $1/32$ is then added to the beginning of the OFDM symbol. It is noteworthy that the OFDM symbol we consider has 5617 complex symbols frequency-multiplexed. The generated signal has a usable bandwidth of 5.57 MHz, as per the ISDB-T$_B$ standard, as shown in Fig. 3, which displays the magnitude of power spectrum density of the generated OFDM signal. The entire signal is confined within the -3 MHz to 3 MHz bandwidth, as expected by the standard, with a minor guard band at the boundaries. The simulation did not convert the OFDM signal to channel frequency because, in practical spectral sensing, the first processing step is converting signals from channel frequency to baseband.

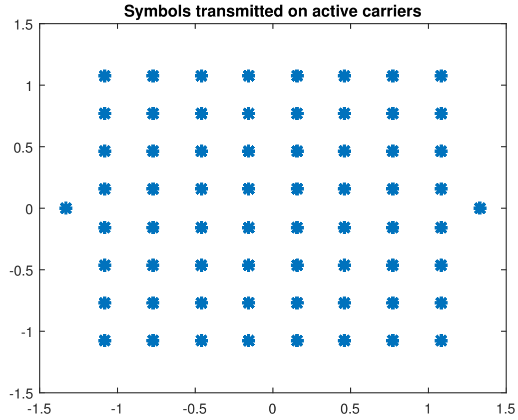

Fig. 2. Symbols transmitted on active carriers.

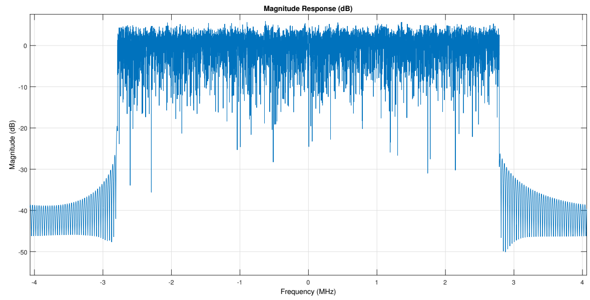

Fig. 3. ISDB-T$_B$ PU signal spectrum.

B. Final Spectral Sensing Simulation in TVWS

To estimate the performance of spectral sensing in a realistic TV White Space scenario, a simulation using MATLAB software was developed. In this simulation, the PU transmission signal, $x(t)$, is that presented in Subsection III-A; the channel gain, $h(t)$, is generated by random samples with a Rayleigh distribution with unit variance, representing a situation of fading where there is no line of sight between CR and PU; and the noise considered, $n(t)$, is the additive white Gaussian noise (AWGN) with zero mean and unitary variance. The sampling frequency used in the simulation is set to match the IFFT clock value indicated in Table I and ensures the detection of all signal power within a 6 MHz channel. The sensing technique considered is energy detection, detailed described in Section II-B. Therefore, the decision variable T, used to define spectral occupancy, is calculated as presented in (2).

The simulation developed has as its main input parameters the number of cooperating CRs (m), the number of samples collected by each CR (n), the number of primary transmitters (p), the signal-to-noise ratio (SNR), the decision threshold, and the number of Monte Carlo events (N_e) used to generate the performance curves.

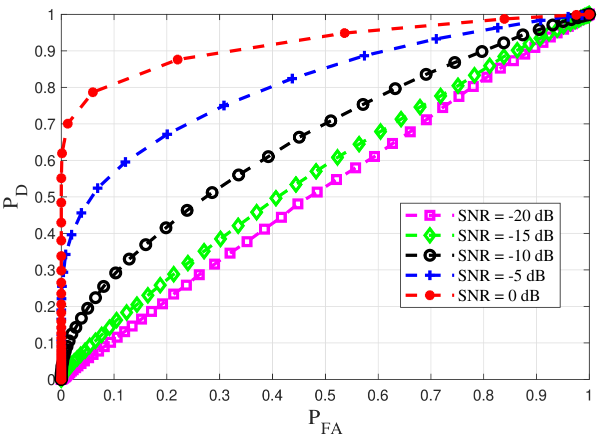

Fig. 4. ROC curves varying the SNR values.

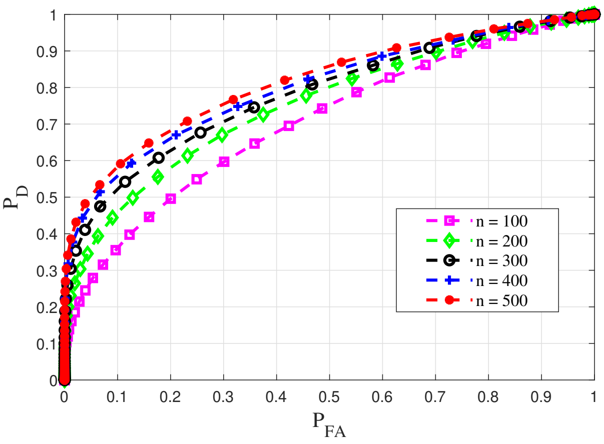

Fig. 5. ROC curves varying the number of samples collected by the CR.

IV. Numerical Results

This section presents the performance results of spectral sensing in various TVWS scenarios. All performance curves presented in this section were obtained through careful simulations developed on the MATLAB software platform, which took into account no less than 15000 Monte Carlo events.

To investigate the impact of different SNR values on the sensing system performance, simulations were conducted with the parameters $p = 1$, $m = 1$, $n = 50$, and SNR levels of -20 dB, -15 dB, -10 dB, -5 dB, and 0 dB. The Receiver Operating Characteristic (ROC) curves for each SNR level were obtained and presented in Fig. 4. The results show that the worst performance is achieved at SNR $= -20$ dB and a significant improvement is observed as the SNR increases towards 0 dB. However, the analysis of the curves highlights that in a TVWS scenario using energy detection sensing techniques, obtaining reliable results for low SNR values and with a limited number of collected samples (as in this first case study, where $n = 50$) in an NLOS scenario is practically unfeasible since an operation point where the detection probability tends to 1 and the probability of false alarm tends to zero is far from been achieved even for SNR $=$ 0 dB.

To assess the impact of the number of samples, n, collected by the CR on the spectral sensing system, a new simulation was conducted with the following parameters: $p = 1$, $m = 1$, SNR $= -10$ dB, and $n = 100$, 200, 300, 400, and 500. The simulation results are presented in Fig. 5, revealing that the number of samples collected by the CR is a critical factor in improving sensing performance. Specifically, a higher number of samples yields a ROC curve closer to the optimal point, providing more information about the sensed band and enabling more reliable detection of PU transmissions. These findings suggest that in practical sensing in TVWS scenarios, the number of samples collected by the CR should be sufficiently large, exceeding even 500 samples, to ensure that the probabilities of detection and false alarm remain within the acceptable limits of the developed sensing system.

In practical spectral sensing projects using energy detection, the decision threshold used for comparison with the decision variable is calculated according to equation (5), taking into account the false alarm probability that can be tolerated by the system. To assess the behavior of the probability of detection for a fixed false alarm probability and various SNR values, a new sensing simulation was performed with the following configuration: $p = 1$, $m = 1$, $n = 1000$, and SNR varying from -20 to 0 dB. Four different thresholds were used, each with a corresponding false alarm probability: $\lambda = 1098$ ($P_{\text{fa}} = 0.1\%$), $\lambda = 1073$ ($P_{\text{fa}} = 1\%$), $\lambda = 1052$ ($P_{\text{fa}} = 5\%$), and $\lambda = 1040$ ($P_{\text{fa}} = 10\%$), and were calculated based on equation (5). The results are presented in Fig. 6, which demonstrates that the obtained false alarm probability is consistent with the theoretical expectations for each threshold case. Furthermore, it shows that as the system is allowed to operate with a higher false alarm probability, the probability of detecting a primary user in the sensed band increases. A crucial conclusion drawn from this analysis is that even when increasing the number of collected samples to $n = 1000$, for SNR values lower than 0 dB, none of the evaluated curves approach a probability of detection of 100%. This is only achieved close to an SNR of 5 dB, indicating that in a real-world TVWS scenario where the CR may be in a shadowed environment or severe fading condition, the number of samples should be even higher than what was used in this analysis. Alternatively, if this is not feasible, another sensing technique or cooperative sensing should be considered.

To complement the analysis, a final performance evaluation is presented considering a cooperative sensing scenario in TVWS, in which each CR of the cooperative network collects n samples and sends them to a fusion center (FC), where the test statistic is calculated considering the samples collected by all radios. For this purpose, the simulation considered the following parameters: $p = 1$, $n = 50$, SNR $= -10$ dB, and $m = 1$, 2, 3, 4, and 5. The simulation results are presented in Fig. 7. After analyzing the curves presented in Fig. 7, it can be concluded that spectral sensing performance improves as the number of radios used to collect samples increases. This improvement is due to the increase in the total number of collected samples, which leads to a proportional increase in the number of processed samples at the FC. Additionally,

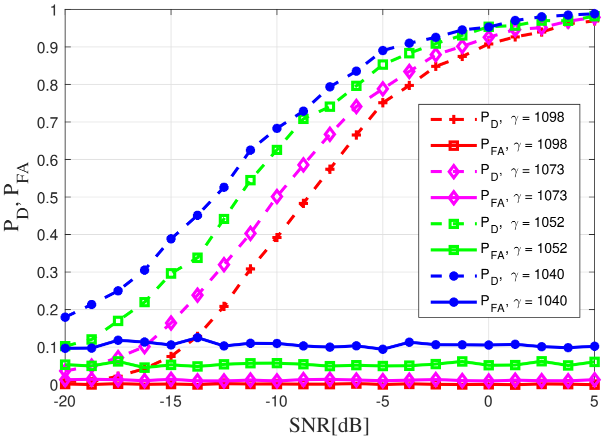

Fig. 6. P_d and P_{fa} versus the SNR.

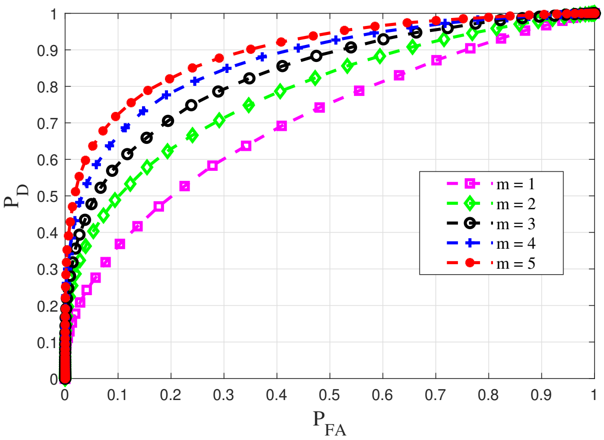

Fig. 7. ROC curves varying the number of CRs.

the samples collected by each remote radio are spatially uncorrelated, which reduces uncertainty in the channel analysis. However, the practical implementation of this cooperative sensing approach is much more complex compared to non-cooperative sensing, as it requires multiple remote radios and a fusion center that communicates with all remote radios in the network and manages the spectral allocation of available free channels.

V. Conclusions

In conclusion, this article contributes to the investigation of energy detection-based spectrum sensing for TV White Space scenarios in Brazil. It provides valuable insights into the optimization of spectrum sensing systems in TVWS scenarios by simulating a primary user signal under realistic settings and considering the receiver signal with fading. Our findings demonstrate the importance of considering various parameters in achieving robust and reliable sensing, especially in the context of an NLOS fading scenario. Increasing the number of samples collected by cognitive radios in a non-cooperative situation is essential in low SNR situations to achieve satisfactory performance. If this is not possible, employing other more robust detection techniques should be considered. Furthermore, it has also been demonstrated that multiple CRs in a cooperative sensing scenario in TVWS can significantly improve detection quality by adding spatial diversity, albeit with the disadvantage of a more complex implementation. Future work will focus on developing the simulated system using software-defined radio (SDR) and validating other modern techniques of spectral sensing in TVWS. These findings can guide the development of more efficient and reliable TVWS communication systems.

References

[1] P. Newman, "How internet of things technology growth is reaching mainstream companies and consumers," Business Insider, Tech. Rep., Fev. 2020, Access in March 2023. [Online]. Available: https://www.businessinsider.in/tech/news/iot-report-how-internet-of-things-technology-growth-is-reaching-mainstream-companies-and-consumers/articleshow/73925796.cms

[2] P. Cai and Y. Zhang, "Intelligent cognitive spectrum collaboration: Convergence of spectrum sensing, spectrum access, and coding technology," *Intelligent and Converged Networks*, vol. 1, no. 1, pp. 79–98, 2020.

[3] H. B. Sandya, K. Nagamani, and L. Shavanthi, "A review of cognitive radio spectrum sensing methods in communication networks," in *2018 International Conference on Communication and Signal Processing (ICCSP)*, 2018, pp. 0457–0461.

[4] "Resolução ANATEL Nº 747," Conselho diretor Anatel, 10/2021, 2021, Access in April 2023. [Online]. Available: https://www.gov.br/anatel/pt-br/assuntos/noticias/anatel-publica-resolucao-para-uso-de-espectro-ocioso

[5] M. Ali, M. N. Yasir, D. M. S. Bhatti, and H. Nam, "Optimization of spectrum utilization efficiency in cognitive radio networks," *IEEE Wireless Communications Letters*, vol. 12, no. 3, pp. 426–430, 2023.

[6] V. Amrutha and K. V. Karthikeyan, "Spectrum sensing methodologies in cognitive radio networks: A survey," in *2017 International Conference on Innovations in Electrical, Electronics, Instrumentation and Media Technology (ICEEIMT)*, 2017, pp. 306–310.

[7] A. Ali and W. Hamouda, "Advances on spectrum sensing for cognitive radio networks: Theory and applications," *IEEE Communications Surveys & Tutorials*, vol. 19, no. 2, pp. 1277–1304, 2017.

[8] L. Zhang, M. Zhao, C. Tan, G. Li, and C. Lv, "Research on spectrum sensing system based on composite neural network," in *2020 2nd International Conference on Advances in Computer Technology, Information Science and Communications (CTISC)*, 2020, pp. 22–26.

[9] M. Oner and F. Jondral, "Cyclostationarity based air interface recognition for software radio systems," in *Proceedings. 2004 IEEE Radio and Wireless Conference (IEEE Cat. No.04TH8746)*, 2004, pp. 263–266.

[10] Y. Zeng, Y.-C. Liang, A. T. Hoang, R. Zhang, and Z. Liu, "A review on spectrum sensing for cognitive radio: Challenges and solutions," *EURASIP Journal on Advances in Signal Processing*, 2010.

[11] W. Zhao, H. Li, M. Jin, Y. Liu, and S.-J. Yoo, "Eigenvalues-based universal spectrum sensing algorithm in cognitive radio networks," *IEEE Systems Journal*, vol. 15, no. 3, pp. 3391–3402, 2021.

[12] Y. Arjoune and N. Kaabouch, "A comprehensive survey on spectrum sensing in cognitive radio networks: Recent advances, new challenges, and future research directions," *Sensors*, vol. 19, no. 1, 2019.

[13] H. Huang and C. Yuan, "Cooperative spectrum sensing over generalized fading channels based on energy detection," *China Communications*, vol. 15, no. 5, pp. 128–137, 2018.

[14] W. Wu, Z. Wang, L. Yuan, F. Zhou, F. Lang, B. Wang, and Q. Wu, "Irs-enhanced energy detection for spectrum sensing in cognitive radio networks," *IEEE Wireless Communications Letters*, vol. 10, no. 10, pp. 2254–2258, 2021.

[15] C. Vlădeanu, A. Marţian, and D. C. Popescu, "Spectrum sensing with energy detection in multiple alternating time slots," *IEEE Access*, vol. 10, pp. 38 565–38 574, 2022.

[16] D. M. M. Plata and Á. G. A. Reátiga, "Evaluation of energy detection for spectrum sensing based on the dynamic selection of detection-threshold," *Procedia Engineering*, vol. 35, pp. 135–143, 2012.

[17] "Televisão digital terrestre - Sistema de transmissão," Associação Brasileira de Normas Técnicas - ABNT 15601, Rio de Janeiro, 2007, Access in November 2022. [Online]. Available: https://www.normas.com.br/visualizar/abnt-nbr-nm/26689/nbr15601-televisao-digital-terrestre-sistema-de-transmissao